Yurchenko et al., https://doi.org/10.1083/jcb.201707027

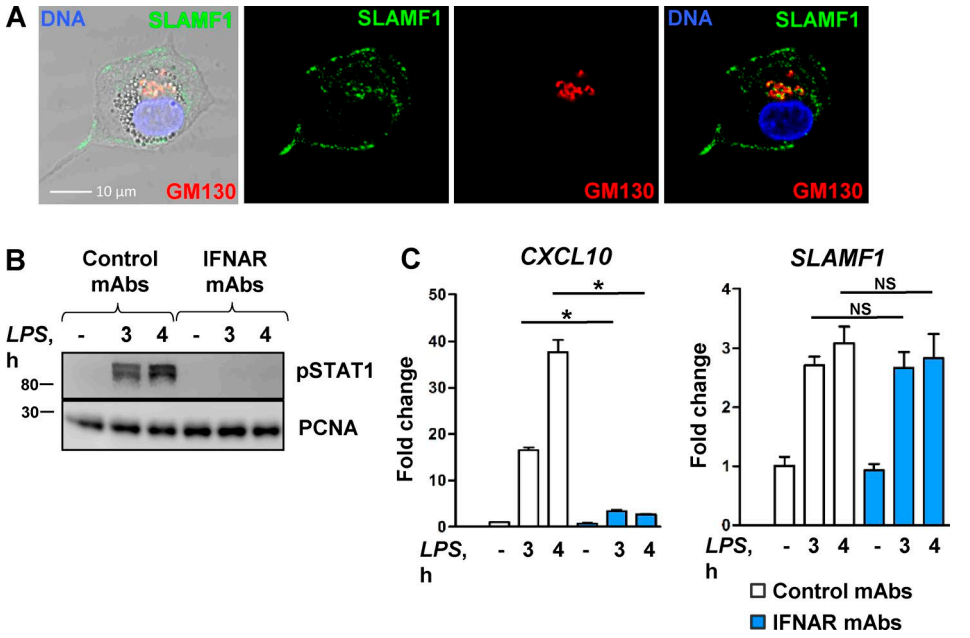

Figure S1. **LPS treatment induces SLAMF1 expression in human cells, resulting in its surface localization, and the increase in SLAMF1 expression is not dependent on signaling from the IFNAR. (A)** SLAMF1 staining in human monocytes after 6 h of LPS stimulation. Middle z stacks of confocal images of a representative cell stained by anti-SLAMF1 and anti-GM130 (Golgi marker) antibodies as well as Hoechst (nuclear staining). **(B and C)** Cells were preincubated for 30 min with control mAbs (MOPC-173) or IFNAR chain 2 mAbs before addition of LPS for 3 and 4 h. Lysates were used for simultaneous isolation of RNA and protein. (B) Proteins were analyzed by Western blot analysis for pSTAT1 (Y701) levels, and PCNA Western blot was used as a loading control. Molecular weight is given in kilodaltons. (C) qPCR data of *SLAMF1* and *CXCL10* mRNA expression from the same experiment as in B. Western blot results are representative of one independent experiment out of three. Error bars represent means ± SD for data from three independent experiments. Statistical significance was evaluated by a two-tailed *t* test. *, $P < 0.001$.

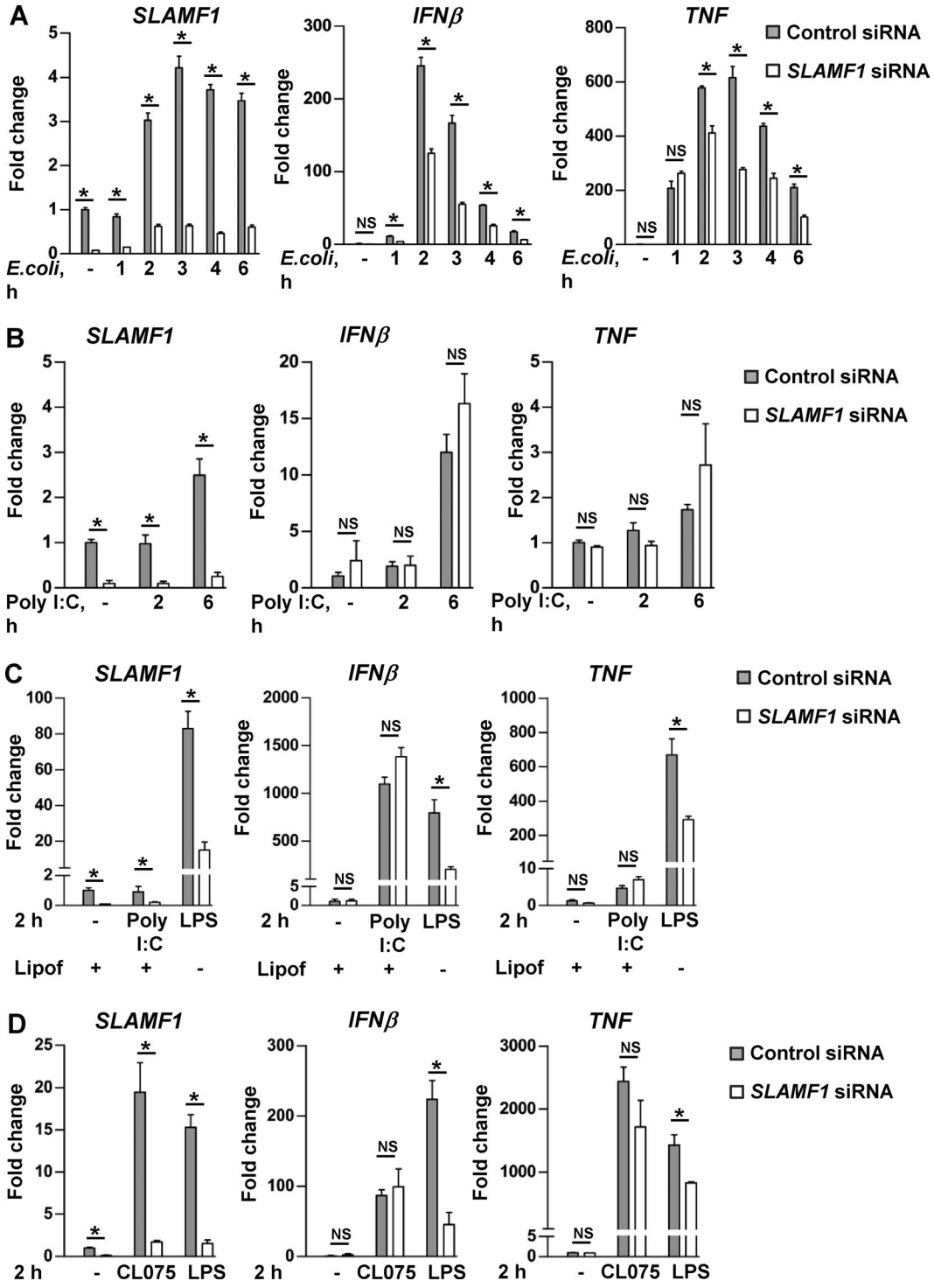

Figure S2. **SLAMF1 is involved in the regulation of TLR4 (*E. coli*– or LPS-)-mediated but not TLR3-, TLR8-, or RIG-1/MDA-5–mediated *IFNβ* or *TNF* mRNA expression. (A)** qPCR data of *SLAMF1*, *IFNβ*, and *TNF* mRNA expression for THP-1 cells cocultured with *E. coli* particles for indicated time points representative of three independent experiments. **(B–D)** Human macrophages silenced by control or SLAMF1 siRNA and treated with poly I:C (20 µg/ml) for 2 and 6 h (B), transfected poly I:C using Lipofectamine 3000 (Lipof) or LPS (100 ng/ml) for 2 h (C), or by CL075 (1 µg/ml) or LPS for 2 h (D). Results are representative of three donors. Error bars show means ± SD for biological replicates. Statistical significance was evaluated by a two-tailed *t* test. *, $P < 0.01$.

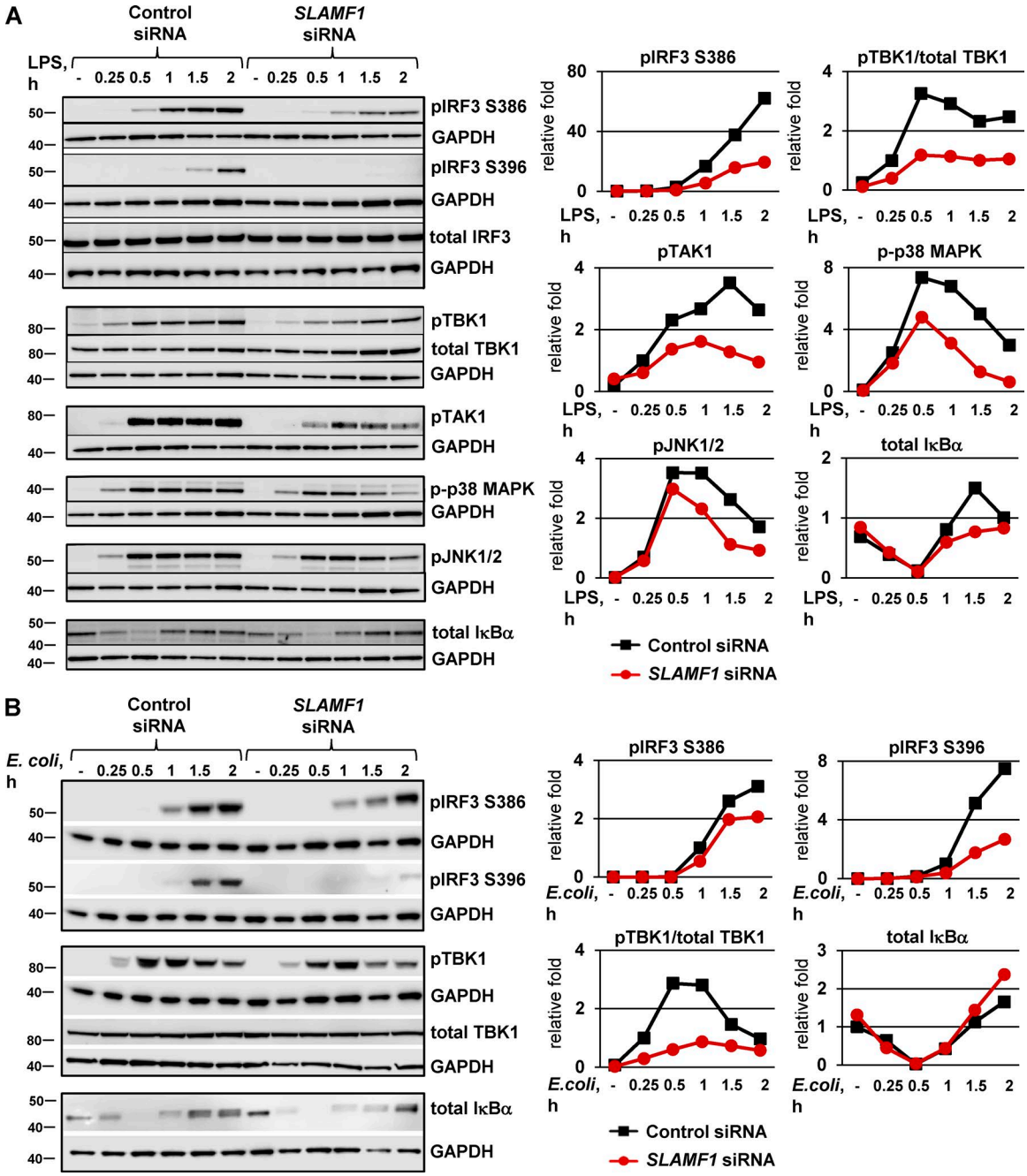

Figure S3. **Knockdown of SLAMF1 in THP-1 cells impairs TLR4-mediated phosphorylation of TBK1, IRF3, and TAK1 in response to ultrapure LPS or *E. coli* particles. (A and B)** Western blot analysis of lysates from THP-1 cells (representative experiment) treated with control oligonucleotides or *SLAMF1*-specific siRNA oligonucleotides and stimulated by ultrapure LPS (A) or *E. coli* particles (B). The same GAPDH controls are presented for total IRF3 and total IκBα, for pIκBα and pTAK1 (A), and for pIRF3 S396 and pTBK1 (B) because they were probed on the same membranes. Graphs (right) show quantifications of protein levels relative to GAPDH levels if not stated otherwise on the title. Quantifications were performed with Odyssey software. Five independent experiments were performed for each treatment condition with almost identical results. Molecular weight is given in kilodaltons.

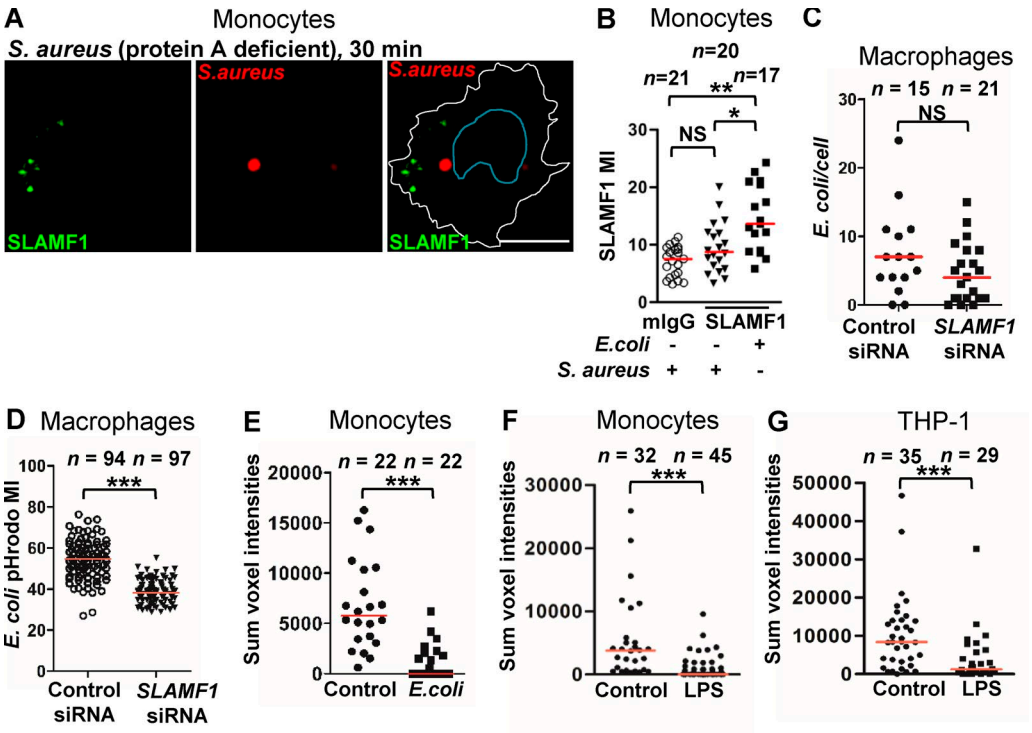

Figure S4. **SLAMF1 relocalizes from ERCs to early and late *E. coli* phagosomes but not *S. aureus* phagosomes and is required for *E. coli* phagosome acidification in human cells. (A)** Human monocytes incubated for 30 min (pulse-chase: 15 min + 15 min) with *S. aureus* and *E. coli* pHrodo particles, fixed, and stained for SLAMF1 with representative images for *S. aureus*–treated cells. Bar, 10 µm. **(B)** Quantification of SLAMF1 MIs around *S. aureus* and *E. coli* phagosomes using ImageJ/Fiji software. **(C and D)** Numbers of *E. coli* particles uptake per cell (C) and MIs for *E. coli* pHrodo particles (D) in macrophages silenced by control or *SLAMF1* siRNA coincubated with particles for 30 min. **(E–G)** Cells were treated by AF488 *E. coli* particles (E) for 30 min or ultrapure LPS (F and G) for 1 h, followed by immunostaining for GM130 and SLAMF1 and z stack imaging on a confocal microscope. Sum of voxel intensities for SLAMF1 staining inside individual GM130 "rings" was quantified using ImageJ/Fiji software. Data are representative of at least three independent experiments. Statistical analysis was performed using a Mann-Whitney test. Lines in the plots represent medians, and *n* = number of observations. *, $P < 0.01$; **, $P < 0.001$; ***, $P < 0.0001$.

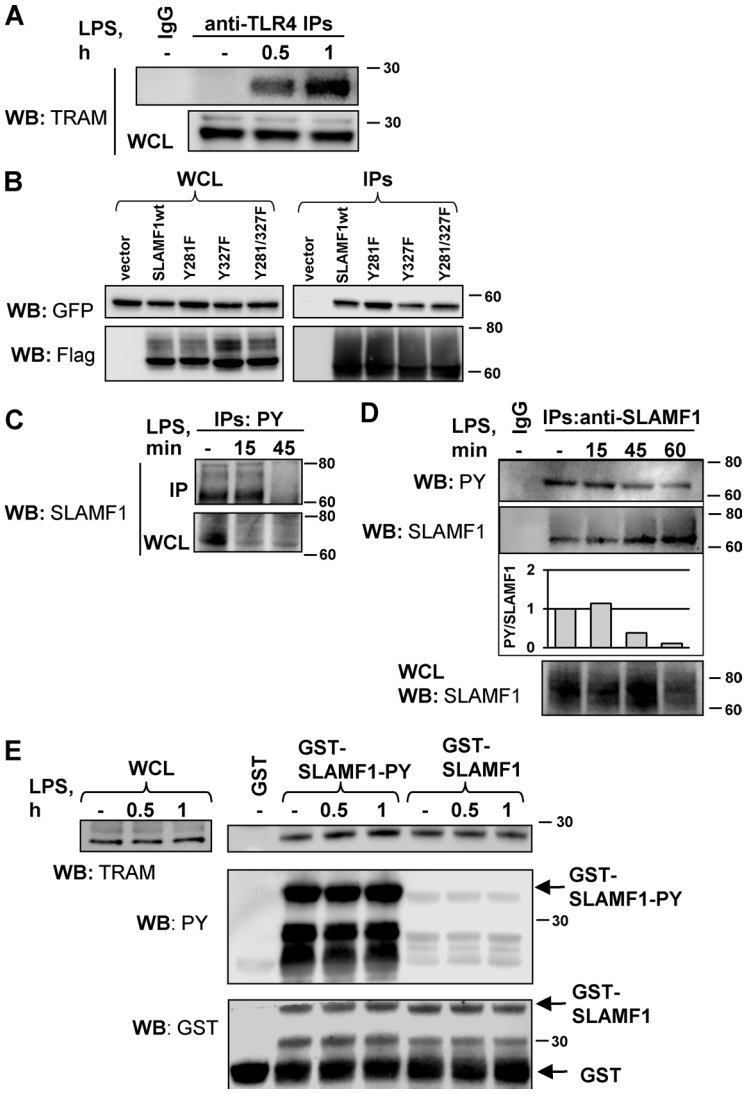

Figure S5. **SLAMF1 interaction with TRAM is independent from SLAMF1 tyrosine phosphorylation. (A)** A TRAM band of expected size was detected after LPS stimulation of macrophages using specific anti-TRAM antibodies in endogenous TLR4 IPs by anti-TLR4 antibodies. **(B)** Coprecipitations of SLAMF1^{Flag} with point mutations Y281F, Y327F, and Y281/327F with TRAM^{YFP}. **(C)** Endogenous IPs with antiphosphotyrosine (PY)-biotinylated antibodies followed by precipitation with streptavidin beads and anti-SLAMF1 Western blot (WB) analysis. **(D)** Anti-SLAMF1 IPs followed by antiphosphotyrosine and anti-SLAMF1 Western blotting. Anti-IgG control IP was performed from the same amount of lysate of nonstimulated cells (no LPS). The graph represents relative numbers for phosphotyrosine band density values obtained in Odyssey software and normalized to total SLAMF1 levels in IPs. **(E)** GST pulldown assays from lysates of macrophages stimulated by LPS at different time points followed by Western blot analysis for TRAM. Antiphosphotyrosine Western blotting was performed to control tyrosine phosphorylation of GST-SLAMF1-phosphotyrosine–recombinant protein, and anti-GST Western blotting was performed for loading controls of fusion proteins. Endogenous IPs and GST pulldown assays were performed from lysates of primary human macrophages differentiated for 10 d. Data are representative of at least three independent experiments. Molecular weight is given in kilodaltons. WCL, whole-cell lysate.

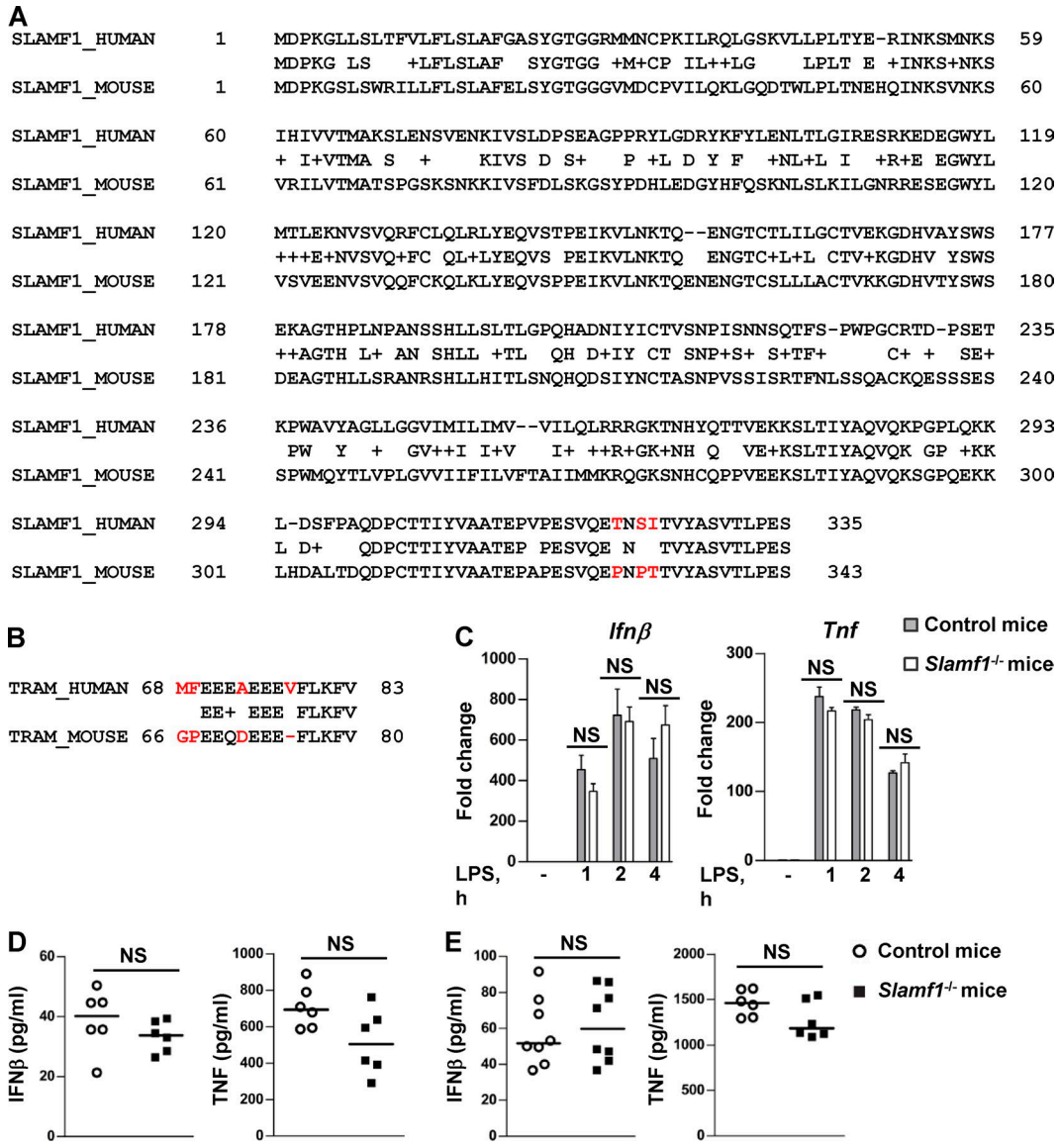

Figure S6. **TLR4-mediated *IFNβ* and *TNF* mRNA expression and cytokines' secretion were not altered in *Slamf1*$^{-/-}$ BMDMs. (A and B)** Full sequence alignment of human and murine SLAMF1 proteins (A) and partial alignment of human and murine TRAM proteins in the SLAMF1-interacting domain (B). Amino acids different in murine and human proteins within SLAMF1ct–TRAM interaction domains are marked by red. **(C)** *Ifnβ* and *Tnf* mRNA levels by qPCR in control and *Slamf1*$^{-/-}$ BMDMs stimulated by ultrapure LPS (100 ng/ml). Error bars represent means ± SD for combined data from six independent experiments. A two-tailed *t* test was applied to evaluate statistical significance. **(D and E)** Quantification of IFNβ and TNF secretion levels in control and *Slamf1*$^{-/-}$ BMDMs stimulated by ultrapure LPS (D) or *E. coli* particles (E) for 6 h accessed by ELISA. BMDMs isolated from six mice both for control and *Slamf1*$^{-/-}$ mice. One dot on the graph represents the median value of three independent experiments for BMDMS from each mouse. Statistical analysis was performed using a Mann-Whitney test.

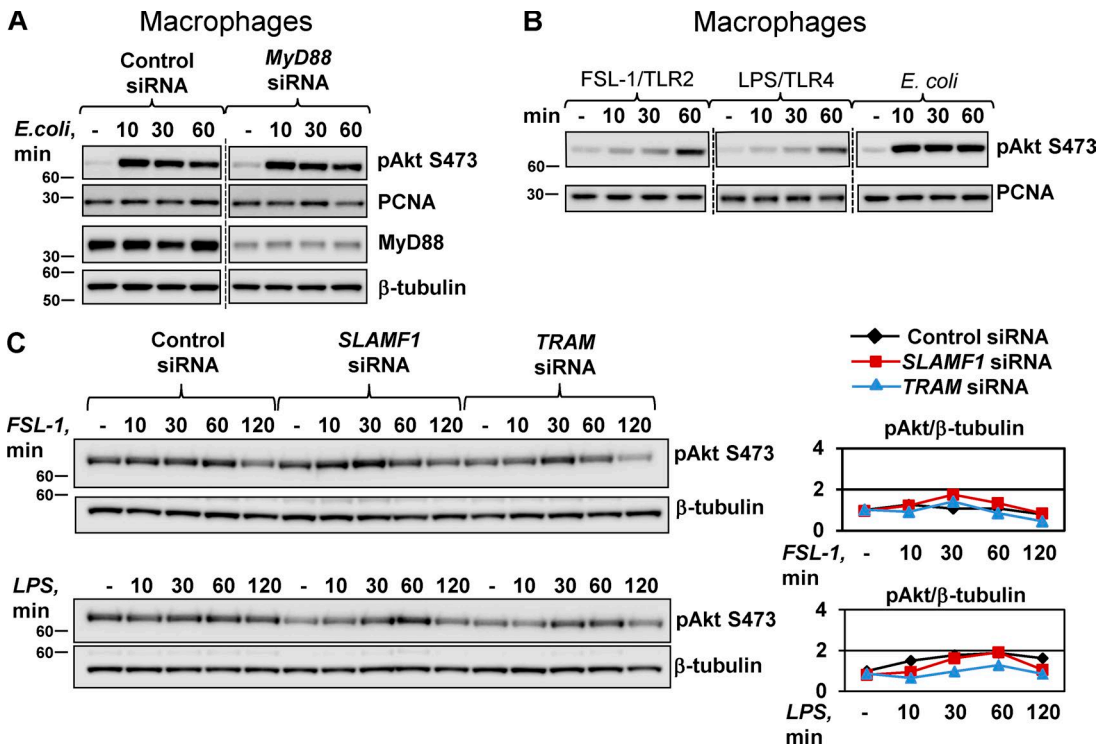

Figure S7. ***E. coli*–mediated Akt phosphorylation in macrophages is not dependent on MyD88 expression, and TLR2- and TLR4-induced phosphorylation of Akt is weak and not much dependent on *SLAMF1* or *TRAM* expression. (A)** pAkt (S473) levels in human macrophages silenced by control siRNA or *MyD88* siRNA. *MyD88* silencing was assessed by anti-MyD88 Western blotting. Images in A show different parts of the same membranes. **(B and C)** Western blot analysis of pAkt in lysates from primary macrophages (B) and THP-1 cells (C) stimulated by FSL-1 (20 ng/ml), K12 LPS (100 ng/ml), or *E. coli* particles (20/cell; B) for various time points. Images in B show different parts of the same membranes. THP-1 cells were pretreated with control, *SLAMF1*-, or *TRAM*-specific siRNA before stimulation (B). PCNA (A and B) or β-tubulin (A–C) were used as loading controls. Dashed lines indicate that intervening lanes have been spliced out. Quantification of pAkt (S473) levels (C) was performed with Odyssey software and correlated to basal levels of pAkt and loading controls (right). Molecular weight is given in kilodaltons.